Chapter 6

Denial-of-Service Attack Resilient Control for Autonomous AC microgrid

This chapter is dedicated to attaining another objective of the thesis work that is resilient control design against the cyber threat in the microgrid power network. In a microgrid network system, cyber resiliency is a prerequisite for smooth operation under cyber threats. Denial of service (DOS) in microgrid based network systems has high probable cyber threat where system stability is challenged by the interruption in the communication on control signal to actuator or on the measurement of sensor data to the controller. In this chapter input to state stability (ISS) of closed loop microgrid system is preserved by characterizing the DOS duration and frequency. ISS of the microgrid system is achieved under DOS through the determination of adequate arrangement in transmission triggering. The event trigger analysis with suitable inequality is presented both in absence and presence of DOS attack to make the controller design practically possible for the secondary voltage-frequency regulation in an autonomous ac microgrid. The law for updated control propagation is determined by the sliding mode control analysis. Lyapunov function is used to analyze the stability of microgrid systems under sequence of DOS attack. The DOS based cyber resiliency of proposed scheme is verified in MATLAB/Simulink environment.

6.1 Introduction

The software in closed loop controls as well as communication networks enhances susceptibility for cyber conciliations in the microgrid [120], [121]. Microgrids are progressively initiated to renovate into cyber-physical microgrids including distributed and decentralized multi-agent features using advanced power electronics [122].

The AC microgrid distributed cooperative control [123]-[125] has now arisen as an alternative to centralized control as it provides improved robustness and smooth control

capabilities. In these control strategies inverters are considered as nodes in a sparse communication digraph. Through the communication digraph it is ensured that all nodes will reach a common consensus as per measures delivered by the reference node.

Microgrid control strategies involve three layers of hierarchical structures of control that are primary, secondary, and tertiary in order to achieve smooth and stable operation [126]. In primary control procedure, distributed generations (DGs) have local control loops that are based on the droop control operation. Integrated DGs are the main building component of microgrid that efficiently facilitate the small-scale power system [127],[128]. One of the primary control objectives is to take care of frequency and voltage regulation and maintain stability when the microgrid goes in islanded mode. In general, microgrids have two modes of operation that are grid connected and islanded mode of operation [128], [129]. Secondary control is followed by the primary operation in hierarchical control structure of microgrid to further restore voltage and frequency that may be deviated due to disturbances and system uncertainties [128], [129], [130]. It provides reference to all DGs primary control connected through a common bus. Hence cyber threat in secondary control layer in practical circuits may introduced due to involvement of communication network in between the bus interconnections. Cyber-physical networks (CPNs) in the previous decade have the center of attention to research community that is evolved from the integration of networking, computation, and physical procedures [131]. Due to interconnection of cyber components of microgrid with its physical properties under CPNs environment may introduce various aspect to analysis such as fault [132], observer design [133], security issues [134], [135] and stability bounds [136], [137].

In most of the existing control concern is focused on the uncertainty and fault compensation which causes failure of communication in the network control tactics [138], [139]. These approaches do not effectively cover the malicious cyber adversary. Especially in CPNs cases, where physical parameters are interacted with cyber component and hence vulnerable to cyber intimidations. The main classification of attacks in microgrid communication link are deception and DOS attacks. Deception attack is

concerned with the data reliability by influencing transmitted packets over the communication network [140]– [144], whereas DOS attacks primarily planned to loss packets in a way to disrupt the exchange of information timeline [145], [146]. Investigation on DOS attacks that interrupt the communication availability in microgrid networks are limited. The effect of DOS attack in [147], is investigated on microgrid communication network by game theory approach using phasor measurement units. Similarly [148], describes the impact of DOS attack on frequency in microgrid secondary control operation. In both [147] and [148], it is shown that the DOS attack upsets microgrid stability by avoiding restoration process of secondary controller. An auxiliary communication interface of power line is utilized in network reconfiguration method in [149], to overcome the impact of DOS attack. To extend the resiliency of microgrid in islanded mode of operation against DOS attack, a fallback control in [150] is applied for energy storage. Although these algorithms against DOS attack in microgrid are much impactful and promising but lacks to present solid microgrid stability assessment during DOS attack which is a key role for an algorithm against DOS [151], [152]. In this chapter a control scheme based on sample data is considered for DOS attack in microgrid communication network. The DOS attacker intended to introduce instability in the controller by preventing communication on control signal to actuator or on the measurement of sensor data to the controller channels. In open loop process develops the control as per the last transmitted sample during DOS attacks, whereas in close loop microgrid configuration the point of interest is to determine close loop bounds to preserve stability in some predefined sense. Pertaining to this DOS attack modelling is an issue of concern. In previously reported work it is difficult to explain the problematic packet drop stimulation for a DOS attacker. This chapter follows a simple model of DOS attack where attacker can target the time constraints only in the form of DOS attack duration and its frequency. This configuration of DOS attack can cover various DOS attacks like periodic, trivial, random, and jamming attacks [153]– [155].

In this chapter microgrid stability under DOS attack is preserved by characterizing the duration and frequency of DOS attack in the sense of relating stability with the jamming

on-off periods [156].

The main contribution of the chapter is addressed as:

- The norms of data transmission event are determined by satisfying the stability condition through the Lyapunov stability criteria for on-off DOS attack periods. In this way ISS of microgrid under DOS attack is ensured.
- Robustness of multi DGs based microgrid system against disturbances in secondary control design is maintained by siding mode control design.

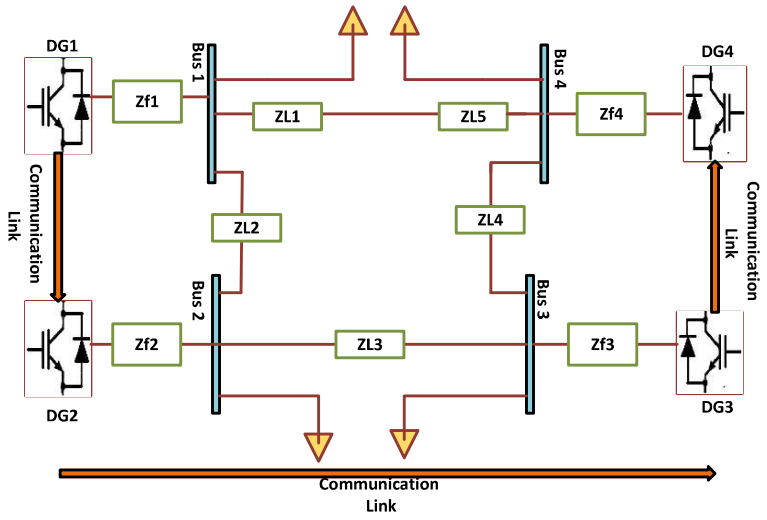

Figure 6.1. Multi DG based microgrid structure.

6.2 Microgrid control design for DOS attack

The multi-DG based microgrid structure is shown in Figure *6.1*. In this configuration power electronic DC/AC converters are used to integrate distributed generators (DG's) to ac buses. The interconnected DGs includes primary power source & inner current- voltage control loops. This primary control provides output voltage-frequency regulation [157], with their reference dq reference frame. To achieve tracking synchronization with the reference DG, other DGs primary control reference must follow the consensus based secondary control. To fulfil this objective, each DGs voltage magnitude is linked with d-axis of the reference value. Therefore, i^{th} DGs d-axis voltage component can be written as [158]:

$$\begin{cases} v_{odi}^{*} = V_{ni} - n_{Qi}Q_i \\ v_{oqi}^{*} = 0 \end{cases} \quad 6.1$$

The V_{ni} represents secondary voltage control so that ($v_{omag} \rightarrow v_{ref}$)[158]. Where terminal output magnitude (v_{omag}) of DG voltage is written as:

$$v_{omag} = \sqrt{v_{odi}^2 + v_{oqi}^2} \tag{6.2}$$

Similarly, the i^{th} DGs frequency has to follow the secondary frequency as ($\omega_i \rightarrow \omega_{ref}$). The dynamics of i^{th} DG can be given as [158]:

$$\begin{cases} \dot{z}_\iota = f_i(z_i) + k_i(z_i)б_i + g_i(z_i)u_i \\ y_i = h_i(z_i) + d_i u_i \end{cases} \tag{6.3}$$

with, $z_i = \left[\delta_i\ P_i\ Q_i\ \phi_{di}\ \phi_{qi}\ \Upsilon_{di}\ \Upsilon_{qi}\ i_{Ldi}\ i_{Lqi}\ v_{odi}\ v_{oqi}\ i_{odi}\ i_{oqi}\right]^T$, δ_i represents common angle reference of i^{th} DG. P_i denotes active and Q_i denotes reactive output power at filter terminal. ϕ_{di} & ϕ_{qi} denotes auxiliary voltage components whereas Υ_{di} & Υ_{qi} denotes the auxiliary current components. The other parameters like $i_{Ldi}, i_{Lqi}, v_{odi}, v_{oqi}, i_{odi}$, & i_{oqi} are respectively the inverters current, filter output voltage and output current components of i^{th} DG. The $б_i$ in (*6.3*) is the vector of $б_i = \left[v_{com}\ v_{bdi}\ v_{bqi}\right]^T$ as internal AC bus component variables. The value of $y_i = v_{odi}$ & $u_i = V_{ni}$ represents the secondary voltage control. Secondary frequency control is designed as $u_i = \omega_{ni}$ & $y_i = \omega_i$. Rest of the other functions $f_i(z_i)$, $g_i(z_i)$, $h_i(z_i)$ & $k_i(z_i)$ are considered as per [158].

6.3 Control objective under DOS attack

Here the DOS is considered as a phenomenon that is intended to avoid control signal propagated at a desired event. In this chapter it is considered that both the control (actuator signal) and measurement (sensor signal) channels are influenced by the DOS attack simultaneously. Therefore, in this case no exchange of data is executed from the channels. The DOS sequence from off to on is expressed as $\langle h_n \rangle$ with $h_0 \geq 0$. In this DOS sequencing zero means the communication between channels is possible whereas one sequencing represents no communication is possible between channels. Therefore n^{th} time duration of DOS over which no possibility of communication with $\tau_n \in \mathcal{R}$ length is denoted as:

$$H_n = \langle h_n \rangle \cup [h_n, h_n + \tau_n[\tag{6.4}$$

The actuator under DoS attack produces the input signal based on previously updated control signal. The time intervals, $\Xi(\tau,t)$ & $\Theta(\tau,t)$ expressed time set of denial and allowance of communication respectively.

$$\Xi(\tau,t) = \bigcup_{n\in N_0} {}_n\bigcup[\tau,t] \tag{6.5}$$

$$\Theta(\tau,t) = [\tau,t]/\Xi(\tau,t) \tag{6.6}$$

Here the relative complement of $\Xi(\tau,t)$ in $[\tau,t]$ is represented as (*6.6*). Here one need to find an event logic that provide robust action under DOS attack. While designing such a scheme one should ensure a positive away from zero inter execution time of the event-based control logic that is applicable in a physical microgrid network. Therefore, to satisfy it following definitions are adopted:

Definition 1: [159] Any control C˙ obtaining from (*6.3*) will be ISS if β function based on KL-function & γ function based on a K_∞-function exist in a way that,

$$\|x(t)\| = \beta(\|x(0)\|,t) + \gamma\left(\left\|\mathcal{D}_{i_t}\right\|_\infty\right) \tag{6.7}$$

for $\mathcal{D}_i \in \mathcal{L}_\infty$ and microgrid state $x(0) \in \mathcal{R}^n$. Here the values of β and γ are calculated for multi-DG based microgrid as $\beta = \sqrt{\frac{\alpha_2}{\alpha_1}}e^{-\left(\frac{\omega_1}{2}\right)t}$ and $\gamma = \sqrt{\frac{\gamma_4}{\alpha_1\mathcal{L}_1}}$.

Definition 2: The sequence control update $\langle t_k\rangle$ will have property of finite sampling rate if inter execution sampling lower bound rate $\underline{\Delta} \in \mathcal{R}_{(>0)}$ exist in a way that:

$$\Delta_k = t_{k+1} - t_k \geq \underline{\Delta} \tag{6.8}$$

Having $k \in N_0$.

6.3.1. Secondary control

The main objective of the chapter is to achieve tracking synchronization with ISS of all DGs voltage & frequency to the leader reference value through secondary control under DOS attack. In order to achieve this objective, information exchange among neighbouring DGs is required by means of sparse communication, which can be exhibited using graph theory approach. The preliminaries of directed graph theory are addressed in this section 6.3 B.

6.3.1.1. Preliminaries of Graph theory

The edges from j^{th} to i^{th} node is expressed by (v_j, v_i) in the graph theory $\mathrm{G} = (\mathrm{V}, \mathcal{E}, A)$ are communication link between nodes. The N is the number of finite nodes, whereas vertices of graph are represented by $\mathrm{V} = \{v_1, v_2 \ldots v_N\}$. The set of edges are $(\mathcal{E} \subset \mathrm{V} \times \mathrm{V})$. The term of adjacency matrix describing graph pattern is expressed as $A = [a_{ij}] \in \mathcal{R}^{N\times N}$(with a_{ij} as edge (v_j, v_i) weights, a_{ij} is positive if $(v_j, v_i) \in \mathcal{E}$, and $a_{ij} = 0$ is zero otherwise). 'D' as indegree matrix is denoted as $D = diag\{d_i\} \in \mathcal{R}^{N\times N}$ with $d_i = \sum_{j\in N_i} a_{ij}$. Another term in graph theory is the Laplacian matrix 'L' is mathematically represented as $L = D - A$. Spanning tree in graph theory is the direct path between ${i_l}^{th}$ leader node to other nodes.

6.3.1.2. Consensus based voltage error.

Distributed cooperative control is designed to synchronize terminal voltage amplitudes v_{omag} of each DG with reference voltage v_{ref}. By differentiating (*6.1*).

$$\dot{v}_{odi} = \dot{V}_{Ni} - n_{Qi}\dot{Q}_i \equiv u_{vi} \tag{6.9}$$

Here u_{vi} is the auxiliary voltage control that calculates V_{Ni} as per (*6.9*). Now the secondary voltage control of N DG microgrid is featured as first-order linear multi-agent tracking synchronization problem.

$$(\dot{v}_{odN} = u_{vN}) \tag{6.10}$$

$$e_{vi} = \sum_{j\in N_i} a_{ij}(v_{odi} - v_{odj}) + g_i(v_{odi} - v_{ref}) \tag{6.11}$$

The auxiliary control signal u_{vi} are designed based on DG's own information and its neighbor's information through communication graph G, where local neighborhood tracking error is represented as e_{vi}.

6.3.1.3. Consensus based frequency error.

The DG's frequency ω_i synchronizes with the leader node frequency ω_{ref} using control input ω_{Ni}. By differentiating frequency droop characteristic $(\omega = \omega_N - m_p P)$ under nonlinear dynamics (*6.3*) of i^{th} DG yields,

$$\dot{\omega}_i = \dot{\omega}_{Ni} - m_{Pi}\dot{P}_i \equiv u_{\omega i} \tag{6.12}$$

where $u_{\omega i}$ denotes the auxiliary frequency control that facilitates to calculate ω_{Ni} as per (*6.12*). Secondary frequency control of N DG microgrid is featured as first-order linear multi-agent tracking synchronization problem.

$$(\dot{\omega}_N = u_{\omega N}) \tag{6.13}$$

The auxiliary controls $u_{\omega i}$ are designed based on DG's own information and with its neighbor's information through communication digraph G where local neighbourhood tracking error $e_{\omega i}$ is represented as:

$$e_{\omega i} = \sum_{j \in N_i} a_{ij}(\omega_i - \omega_j) + g_i(\omega_i - \omega_{ref}) \tag{6.14}$$

It is stated that all DG's output powers are to be assigned to meet the following equality.

$$m_{P1}P_1 = \cdots = m_{PN}P_N \tag{6.15}$$

where droop coefficients m_{Pi} are chosen as per DGs active power rating. Hence, the secondary frequency control must satisfy (*6.15*). To meet this obligation, an additional control is considered for $m_{Pi}\dot{P}_i$ to regulator synchronization for linear and first-order multi-agent system as (*6.16*) using communication digraph G.

$$\left(m_{PN}\dot{P}_N = u_{PN}\right) \tag{6.16}$$

The auxiliary active power control u_{Pi} is calculated based on own DG information as well as neighbors DG information through the graph with local neighborhood tracking error (e_{Pi}).

$$e_{Pi} = \sum_{j \in N_i} a_{ij}(m_{Pi}P_i - m_{Pj}P_j) \tag{6.17}$$

The consensus error calculated in (*6.11*), (*6.14*) and (*6.17*) are used to achieve auxiliary control u_{vN}, $u_{\omega N}$ and u_{PN} respectively using (*6.18*).

$$\begin{cases} V_{Ni} = \int (u_{vi} + n_{Qi}\dot{Q}_i)dt \\ \omega_{Ni} = \int (u_{\omega i} + m_{Pi}\dot{P}_i)dt \end{cases} \tag{6.18}$$

6.4 Sliding mode-based control strategy.

The multi-DG based microgrid dynamics is written as [158],

$$\begin{cases} \dot{x}_i(t) = u_i(t) + \mathcal{D}_i(t) \\ \dot{x}_l(t) = u_l(t) \end{cases} \quad 6.19$$

Where, $x_i(t) \in \mathcal{R}^n$ is the representation of microgrid states of i^{th} DG as frequency, active power, and direct terminal voltage [158]. The auxiliary control input is $u_i(t) \in \mathcal{R}^n$. The unmodelled bounded disturbance of i^{th} DG is denoted as $\mathcal{D}_i(t) \in \mathcal{R}^n$ having $\|\mathcal{D}_i\| \leq D_i$. The leader state vector is $\dot{x}_l(t) \in \mathcal{R}^n$ and $u_l(t) \in \mathcal{R}^n$ is the leader control input. The aim of the chapter is to model dynamic event-based consensus control scheme to mitigate the impact of DOS attack. Let us take $\tilde{x}_i(t) = x_i(t) - x_l(t) + \beth_i$, & $\tilde{u}_i(t) = u_i(t) - u_l(t)$, with $\beth_i$ is the desired state deviation.

$$\dot{\tilde{x}}_i(t) = \tilde{u}_i(t) + \mathcal{D}_i \quad 6.20$$

Lemma 1 [160]: A control system may achieve synchronous tracking for all agents without any disturbances if the process is considered as:

$$\tilde{u}_i(t) = \mathcal{X}_i^{\eta}(t) \quad 6.21$$
$$\mathcal{X}_i(t) = -\sum_{j \in N_i} a_{ij}\left(\tilde{x}_i(t) - \tilde{x}_j(t)\right) + g_i\left(\tilde{x}_i(t)\right)$$

With $0 < \gamma < 1$ & $1 \leq n_i \leq N$, having N number of DGs as agents.

Lemma 2 [160]: According to graph theory concept, $(L + G)$ matrix has $\mathcal{R}\mathrm{e}(\lambda_{eign}(L + G)) > 0$ in multi-DG based microgrid with the possible directed spanning tree. The sliding surfaces will converge if lemma 3 holds.

Lemma 3[160][161]: If any system represented as $\dot{b} = f(b)$, $f(0) = 0$, $b \in U_0 \subset \mathcal{R}^n$ and $\mathcal{V}(b)$ is in the vicinity of equilibrium point in a way that $\dot{\mathcal{V}}(b) + C_1\mathcal{V}^{\alpha}(b) \leq 0$, with $C_1 > 0$ and $0 < \alpha < 1$ so that $\mathcal{V}(b)$ reaches to equilibrium point in a finite duration. This finite duration can be obtained as $(\mathcal{V}^{1-\alpha}(b(0))/C_1(1-\alpha))$.

Assumption 1: For multi-DG microgrid dynamics (*6.20*). An integral surface in (*6.22*) is taken in a way to achieve finite time convergence.

$$S_i(t) = \tilde{x}_i(t) - \int_0^t \mathcal{X}_i^{\eta}(t)\, dt \quad 6.22$$

As $S_i(t) = [S_1(t), S_2(t) \ldots . S_N(t)]^T$ for $i = 1 \ldots N$. Therefore in the reaching phase (*6.23*) is obtained due to $S_i(t) = 0$ & $\dot{S}_i(t) = 0$.

$$\dot{\tilde{x}}_i(t) = \mathcal{X}_i^{\eta}(t) \tag{6.23}$$

A reaching law to get fast convergence is considered as:

$$\dot{S}_i(t) = -k_1|S_i(t)|^{\frac{1}{2}} sign\big(S_i(t)\big) - k_2 S_i(t) \tag{6.24}$$

With sliding mode gains $k_1 = diag\{k_{11}, k_{12} \ldots . k_{1N}\}$ and $k_2 = diag\{k_{21}, k_{22} \ldots . k_{2N}\}$, $k_{ij} > 0$ for $\forall i, j$. The mathematic function $sign\big(S_i(t)\big) = \big[sign\big(S_1(t)\big), sign\big(S_2(t)\big) \ldots . sign\big(S_N(t)\big)\big]^T$. Here the minimum eigen values as $\lambda_{min}(k_1)$ & $\lambda_{min}(k_2)$ can be taken instead of K_1, K_2. The consensus secondary frequency & voltage control is addressed as:

$$\tilde{u}_{yi}(t) = \mathcal{X}_i^{\eta}(t) - k_1|S_i(t)|^{\frac{1}{2}} sign\big(S_i(t)\big) - k_2 S_i(t) - D_i \tag{6.25}$$

with $\tilde{u}_{yi} \rightarrow u_{vN}, u_{\omega N}$ *or* u_{PN}.

6.4.1. Event based SMC scheme in absence of DOS attack.

The triggering norms in absence of DOS is calculated in a way that control update occurs when there is violation in the state error bounds otherwise same input is propagated. The control (*6.26*) retained in between inter execution events $t \in [t^i \,\&\, t_a^i]$.

$$\tilde{u}_{yi}\big(t_a^i\big) = \mathcal{X}_i^{\eta}\big(t_a^i\big) - k_1\big|S_i\big(t_a^i\big)\big|^{\frac{1}{2}} sign\left(S_i\big(t_a^i\big)\right) - k_2 S_i\big(t_a^i\big) \tag{6.26}$$

The triggering error $\xi_i(t)$ is represented as:

$$\xi_i(t) = \left[\mathcal{X}_i^{\eta}\big(t_a^i\big) - k_1\big|S_i\big(t_a^i\big)\big|^{\frac{1}{2}} sign\left(S_i\big(t_a^i\big)\right) - k_2 S_i\big(t_a^i\big) - \left(\mathcal{X}_i^{\eta}\big(t^i\big) - k_1\big|S_i\big(t^i\big)\big|^{\frac{1}{2}} sign\left(S_i\big(t^i\big)\right) - k_2 S_i\big(t^i\big)\right)\right] \tag{6.27}$$

The triggering error $\xi_i(t)$ is zero at the instant $t_a^i = t^i$. Control input is updated if the triggering error $\xi_i(t)$ contravenes a defined threshold otherwise previously updated control is utilized [162].

Theorem 1: If triggering rule (*6.28*) is violated then the control is updated as per (*6.26*).

$$\|\xi_i(t)\| \leq Б \tag{6.28}$$

With $Б < \left(\lambda_{min}(k_1)\|S_i(t)\|^{\frac{1}{2}} + \lambda_{min}(k_2)\|S_i(t)\| - \mathcal{D}_i\right)$.

Proof 1: A Lyapunov candidate is taken to derive triggering condition by the analysis of

system stability in the sense of ISS.

$$\mathcal{V}_1 = \frac{1}{2} S_i^T(t) S_i(t) \tag{6.29}$$

$$\dot{\mathcal{V}}_1 = S_i^T(t) \dot{S}_i(t) \tag{6.30}$$

with $\dot{S}_i(t) = \dot{\hat{x}}_i(t) - \mathcal{X}_i^{\eta}(t)$, now placing (*6.20*) & (*6.26*),

$$\dot{S}_i(t) = \mathcal{X}_i^{\eta}(t_a^i) - k_1 |S_i(t_a^i)|^{\frac{1}{2}} sign\left(S_i(t_a^i)\right) - k_2 S_i(t_a^i) + D_i - \mathcal{X}_i^{\eta}(t) \tag{6.31}$$

$$\dot{S}_i(t) = \xi_i(t) - k_1 |S_i(t)|^{\frac{1}{2}} sign\big(S_i(t)\big) - k_2 S_i(t) + D_i$$

$$\dot{S}_i(t) = \xi_i(t) - k_1 |S_i(t)|^{\frac{1}{2}} sign\big(S_i(t)\big) - k_2 S_i(t) + D_i$$

Hence,

$$\dot{\mathcal{V}}_1 = S_i^T(t) \left[\xi_i(t) - k_1 |S_i(t)|^{\frac{1}{2}} sign\big(S_i(t)\big) - k_2 S_i(t) + D_i\right]$$

$$\dot{\mathcal{V}}_1 \leq \left\| S_i^T(t) \left[\xi_i(t) - k_1 |S_i(t)|^{\frac{1}{2}} sign\big(S_i(t)\big) - k_2 S_i(t) + D_i\right]\right\|$$

It can be written as $sign\big(S_i(t)\big) = \frac{S_i(t)}{\|S_i(t)\|}$.

$$\dot{\mathcal{V}}_1 \leq \|S_i(t)\| \|\xi_i(t)\| - \lambda_{min}(k_2) \|S_i(t)\|^2 + \mathcal{D}_i \|S_i(t)\| \tag{6.32}$$

Hence according to lemma 3, the triggering rule is obtained in (*6.18*).

6.4.2. Event based control in presence of DOS attack.

Now the microgrid close loop control as shown in Figure *6.2* is relied on the update rule via triggering error $\xi_i(t)$. The control update sequence stabilizes the microgrid system states, if $\xi_i(t)$ satisfies the following norms:

$$\|\xi_i(t)\| \leq \sigma \mathcal{L}_1 \|x(t)\| + \sigma \mathcal{L}_1 \|\mathcal{D}_i\|_{\infty} \tag{6.33}$$

With an adequate design parameter $\sigma \in \mathcal{R}_{(>0)}$.

Here the parameter σ is designed such that the sequence of control update taking place at finite triggering rate that satisfies (*6.33*) can be written as:

$$\lambda_{min}(k_2) - \sigma > 0 \tag{6.34}$$

Then, C' is input to state stable.

Lemma 4: In absence of DOS, control update rule having sampling rate is less than or equal to:

$$\bar{\Delta}_{\sigma} := \frac{1}{\vartheta_1}\frac{\sigma \mathcal{L}_1}{(1+\sigma)} \tag{6.35}$$

will satisfy (*6.33*).

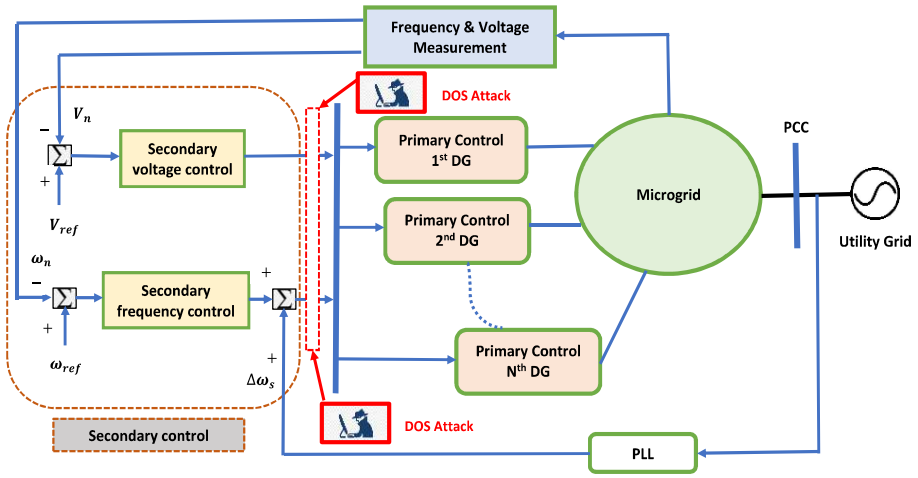

Figure 6.2. DOS attack in secondary control of Multi DG based microgrid.

6.5 DOS attack Preliminaries time limitations

Preliminary objective is to obtain the DOS constraints that the control system is capable of tolerating before violating the stability norms. In this regard an adequate constraint should be employed on the duration & frequency of DOS.

1)Frequency constraint of DOS:

Frequency in terms of occurrence of DOS is to be determine first by defining elapsed time in between two events of DOS as $\mathcal{J}_n = h_{n+1} - h_n, n \in N_0$. From this it is to be observed that if $\mathcal{J}_n < \underline{\Delta}$ for $\forall\, n \in N_0$, (where $\underline{\Delta}$ is the lower bound of sampling rate) the stability of the closed system is preserved under DOS attack. In simple words, for stability subjected to DOS attack frequency of DOS occurrence is to be much lesser than the minimum inter-sampling rate. Now the total number of DOS transitions in a duration $[\tau, t[$, (where $\tau \leq t$) is $n(\tau, t)$ expressed as:

$$n(\tau, t) \leq \xi + \frac{t-\tau}{\partial_D} \tag{6.36}$$

With $\xi \in \mathcal{R}_{(>0)}$ & $\partial_D \in \mathcal{R}_{(>\underline{\Delta})}$.

2)Duration constraint of DOS:

The duration of DOS is concerned with the time interval over which the communication

in microgrid system is denied. The length of this time duration of DOS is expressed as:

$$\Xi(\tau, t) \leq g + \frac{t - \tau}{T} \tag{6.37}$$

With $g \in \mathcal{R}_{(>0)}$ & $T \in \mathcal{R}_{(>1)}$ also $\tau, t \in \mathcal{R}_{(>0)}$ with $t \geq \tau$.

To understand the above DOS attack features the following example is taken and respective features are described. In the example depicted in Figure *6.3* the transitions of DOS attacks are shown. Here the transitions correspond Off to on ($\uparrow$) and on to off transitions ($\downarrow$). The $\uparrow$ transitions in this example are occurred at 4 sec, 9 sec, and 14 sec. The duration of these DOS attacks is respectively 2 sec, 3.5 sec, and 1 sec. The number of attacks in particular durations can be written in this example as: $n(0, 3) = 0$, $n(3, 10) = 2$ & $n(5, 20) = 3$. The duration of DOS defined in the section can be obtained in this example as $\Xi(0, 3) = 0$, $\Xi(2, 11) = [4, 6[\cup [9, 11[$, & $\Xi(11, 20) = [11, 12.5[\cup [14, 15[$.

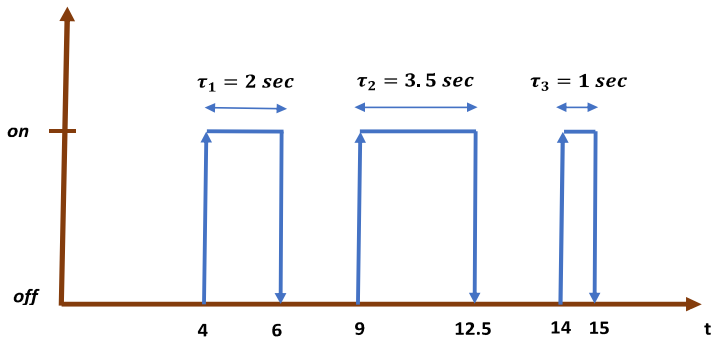

Figure 6.3. Duration and frequency transitions in a DOS signal.

Remark 1: The DOS characteristics discussed above are taken in the chapter for analysis in the microgrid system. Also, in the chapter it has no impact about the available information to the attacker. Therefore, no assumption in this regard is considered on the probable attacker information such as state feedback, process of dynamics and control triggering logic. These kinds of assumptions do not impact widely on the designed control configuration, but the assumption of DOS attack duration & frequency is to be the focus of concern as discussed in this section.

Theorem 2: With consideration of the microgrid control system C constituted by (*6.19*) and having control signal (*6.25*) under the Lyapunov candidate $\mathcal{V}_1 = \frac{1}{2} S_i^T(t) S_i(t)$ serve

as stability analyser. From this the update sequence of the control input with the finite rate of sampling and satisfying the constraint $\mathrm{J}_n < \underline{\Delta}$, and σ as per (*6.33*). Then any of the attack sequence of DOS that satisfies (*6.36*) & (*6.37*) with arbitrary parameters $\mathfrak{z}$, g, ∂_D and T such that following inequality holds:

$$\frac{\Delta_*}{\partial_D} + \frac{1}{T} < \frac{\omega_1}{\omega_1 + \omega_2} \tag{6.38}$$

with Δ_* as a strictly positive value that satisfies the following inequality:

$$\sup_{k \in \varsigma} \Delta_k \leq \Delta_* \tag{6.39}$$

The value of Δ_k is provided in (*6.8*). $\omega_1$is the parameter related to rate of convergence of the close loop microgrid trajectory when the DOS attack is not occurred, whereas ω_2 represents the related parameter to the divergence rate of close loop microgrid trajectory when the DOS attack is occurred. Now the sequence of sampling is taken as $\langle t_k \rangle_{k \in N_0}$ with sequence DoS attack $\langle h_n \rangle_{n \in N_0}$. then

$$\varsigma := \left\{ k \in N_0 | t_k \in \bigcup_{n \in N_0} H_n \right\} \tag{6.40}$$

represents the integer set of microgrid control signal update in presence of DOS attack.

6.5.1. Parameter design for the convergence rate in absence of DOS

Assumption 2: In order to obtain triggering control logic under DOS attack for the microgrid network system (*6.20*), it is assumed that function $f(x_i)$ to its argument is Lipschitz and satisfy the following norm Lipschitz coefficient $\mathcal{L}_1$.

$$\|f(x_i(t)) - \mathfrak{z} f(x_i(t_i))\| < \mathcal{L}_1 \|x_i(t) - x_i(t_i)\| = \mathcal{L}_1 \|\xi_i\| \tag{6.41}$$

Microgrid control dynamics in term of sliding surface is represented in relation to the microgrid state as per the inequality (*6.7*) is written as:

$$\left\| x_i(t) - \int_0^t \mathcal{X}_i^{\eta}(t)\, dt \right\| \leq \|x_i(t)\| \leq \beta(\|x(0)\|, t) + \gamma(\|\mathcal{D}_{ti}\|_\infty)$$

Therefore, the inequality (*6.7*) in terms of sliding surface can be expressed as:

$$\|S_i(t)\| \leq \beta(\|x(0)\|, t) + \gamma(\|\mathcal{D}_{ti}\|_\infty)$$

Similarly, the control triggering rule designed in (*6.28*) can be expressed in terms of state

error per inter execution event by considering assumption (*6.41*).

$$\xi_i(t) = \left[\mathcal{X}_i^{\eta}(t_a^i) - k_1\left|S_i(t_a^i)\right|^{\frac{1}{2}} sign\left(S_i(t_a^i)\right) - k_2 S_i(t_a^i)\right.$$

$$\left. - \left(\mathcal{X}_i^{\eta}(t^i) - k_1\left|S_i(t^i)\right|^{\frac{1}{2}} sign\left(S_i(t^i)\right) - k_2 S_i(t^i)\right)\right]$$

$$\leq \mathcal{L}_1\left(x_i(t_a^i)\right) - \mathcal{L}_1\left(x_i(t^i)\right)$$

Or

$$\xi_i(t) \leq \mathcal{L}_1\left(x_i(t_a^i)\right) - \mathcal{L}_1\left(x_i(t^i)\right) \tag{6.42}$$

Therefore, the condition obtained to stabilize microgrid closed loop plant under DOS attack as per (*6.33*). From (*6.32*), it can be written as:

$$\dot{\mathcal{V}}_1 \leq \|S_i(t)\|\|\xi_i(t)\| - \lambda_{min}(k_2)\|S_i(t)\|^2 + \mathcal{D}_i\|S_i(t)\|$$

Now placing the value of (*6.33*) in (*6.32*) and taking $S_i(t) = \mathcal{L}_1 x(t)$:

$$\dot{\mathcal{V}}_1 \leq \mathcal{L}_1\|x(t)\|(\sigma\mathcal{L}_1\|x(t)\| + \sigma\mathcal{L}_1\|\mathcal{D}_i\|_\infty) - \lambda_{min}(k_2){\mathcal{L}_1}^2\|x(t)\|^2 + \mathcal{D}_i\|x(t)\|$$

or

$$\dot{\mathcal{V}}_1 \leq -(\lambda_{min}(k_2) - \sigma){\mathcal{L}_1}^2\|x(t)\|^2 + \sigma{\mathcal{L}_1}^2\|\mathcal{D}_i\|_\infty\|x(t)\| + \mathcal{D}_i\|x(t)\|$$

or

$$\dot{\mathcal{V}}_1 \leq -(\lambda_{min}(k_2) - \sigma){\mathcal{L}_1}^2\|x(t)\|^2 + \left(1 + \sigma{\mathcal{L}_1}^2\right)\|x(t)\|a(t)$$

where, $a(t) := \sup\{\mathcal{D}_i, \|\mathcal{D}_i\|_\infty\}$, further the above equation can be written as:

$$\dot{\mathcal{V}}_1 \leq -\gamma_1\|x(t)\|^2 + \gamma_2\|x(t)\|a(t) \tag{6.43}$$

With $\gamma_1 = (\lambda_{min}(k_2) - \sigma){\mathcal{L}_1}^2$ and $\gamma_2 = \left(1 + \sigma{\mathcal{L}_1}^2\right)$.

Now applying young's inequality with δ as positive real quantity.

$$2\|x(t)\|a(t) = \frac{1}{\delta}\|x(t)\|^2 + \delta a^2(t) \tag{6.44}$$

By putting $\delta = \frac{\left(1+\sigma{\mathcal{L}_1}^2\right)}{(\lambda_{min}(k_2)-\sigma){\mathcal{L}_1}^2}$ *or* $\frac{\gamma_2}{\gamma_1}$ in (*6.44*), it can be calculated as:

$$\dot{\mathcal{V}}_1 \leq -\frac{\gamma_1}{2}\|x(t)\|^2 + \frac{{\gamma_2}^2}{2\gamma_1}a^2(t) \tag{6.45}$$

The strictly positive Lyapunov function $\mathcal{V}_1$ in terms of microgrid states can be expressed with the state inequality as:

$$\alpha_1 \mathcal{L}_1 \|x(t)\|^2 \leq \mathcal{V}_1(t) \leq \alpha_2 \mathcal{L}_1 \|x(t)\|^2 \quad 6.46$$

From (*6.46*) and (*6.45*) it can be written:

$$\dot{\mathcal{V}}_1 \leq -\omega_1 \mathcal{V}_1\big(x(t)\big) + \gamma_3 a^2(t) \quad 6.47$$

Where, $\gamma_3 = \frac{{\gamma_2}^2}{2\gamma_1}$ and ω_1 as:

$$\omega_1 = \frac{(\lambda_{min}(k_2) - \sigma){\mathcal{L}_1}^2}{2\alpha_2 \mathcal{L}_1} \quad 6.48$$

Here $\|a_t\|_\infty = \left\|\mathcal{D}_{i_t}\right\|_\infty$ for $t \in R_{>0}$. Thus, from (*6.47*) that is the differential inequalities will result in the expression as:

$$\mathcal{V}_1\big(x(t)\big) \leq e^{-\omega_1 t}\mathcal{V}_1\big(x(0)\big) + \gamma_4 \left\|\mathcal{D}_{i_t}\right\|_\infty^2 \quad 6.49$$

Where, $\gamma_4 = \gamma_3/\omega_1$, now from (*6.46*) and (*6.49*) it can be written as:

$$\|x(t)\|^2 \leq \frac{\alpha_2}{\alpha_1} e^{-\omega_1 t}\|x(0)\|^2 + \frac{\gamma_4}{\alpha_1 \mathcal{L}_1}\left\|\mathcal{D}_{i_t}\right\|_\infty^2 \quad 6.50$$

Since it is well known that $a^2 + b^2 \leq (a+b)^2$ for the positive real values of a and b, it can be finally written as:

$$\|x(t)\| \leq \sqrt{\frac{\alpha_2}{\alpha_1}} e^{-\left(\frac{\omega_1}{2}\right)t}\|x(0)\| + \sqrt{\frac{\gamma_4}{\alpha_1 \mathcal{L}_1}}\left\|\mathcal{D}_{i_t}\right\|_\infty \quad 6.51$$

That (*6.51*) is results in the stability bounds as expressed in (*6.7*).

6.5.2. Parameter design for the divergence rate in presence of DOS

The control update in absence of the DOS will be successful. Therefore, according to (*6.42*), the error dynamics will satisfy the following inequality:

$$\begin{aligned} \frac{d}{dx}\|\xi_i(t)\| &\leq \left\|\frac{d}{dx}\xi_i(t)\right\| \\ &\leq \left\|\frac{d}{dx}\left[\mathcal{X}_i^\eta(t_a^i) - k_1\left|S_i(t_a^i)\right|^{\frac{1}{2}} sign\left(S_i(t_a^i)\right) - k_2 S_i(t_a^i)\right]\right\| \end{aligned} \quad 6.52$$

As the previous control remains same during the consecutive events (*6.52*) is obtained.

$$\frac{d}{dx}\|\xi_i(t)\| \leq \left\|\frac{d}{dt}\left[\mathcal{X}_i^\eta(t)\right]\right\| - \left\|\frac{d}{dt}\left[k_1\left|S_i(t)\right|^{\frac{1}{2}} sign\big(S_i(t)\big)\right]\right\| - \left\|\frac{d}{dt}\left[k_2 S_i(t)\right]\right\|$$

$$\frac{d}{dx}\|\xi_i(t)\| \le \eta n^{3-2\eta}\|(L+G)\otimes I_n\|\|\mathcal{X}(t)\|^{2\eta-1}$$

$$-\lambda_{min}(k_1)\left\|\left(tanh\left(ßS_i(t)\right)\frac{d}{dt}\left[|S_i(t)|^{\frac{1}{2}}\right]+|S_i(t)|^{\frac{1}{2}}\frac{d}{dt}\left[sign\left(S_i(t)\right)\right]\right)\right\|$$

$$-\lambda_{min}(k_2)\left\|\dot{S}_i(t)\right\|$$

$$\frac{d}{dx}\|\xi_i(t)\| \le \eta n^{3-2\eta}\|(L+G)\otimes I_n\|\|\mathcal{X}(t)\|^{2\eta-1}$$

$$-\lambda_{min}(k_1)\left(\left\|tanh\left(ßS_i(t)\right)\frac{d}{dt}|S_i(t)|^{\frac{1}{2}}\right\|\right.$$

$$\left.+\|S_i(t)\|^{\frac{1}{2}}\left\|\left(1-tanh^2\left(ßS_i(t)\right)\right)ß\dot{S}_i(t)\right\|\right)-\lambda_{min}(k_2)\left\|\dot{S}_i(t)\right\|$$

Now taking $\left\|\left(1_{n\times n}-tanh^2\left(ßS_i(t)\right)\right)\right\| \le \|1_{n\times n}\| = n$

$$\frac{d}{dx}\|\xi_i(t)\| \le \eta n^{3-2\eta}\|(L+G)\otimes I_n\|\|\mathcal{X}(t)\|^{2\eta-1}$$

$$-\lambda_{min}(k_1)\left(\left\|tanh\left(ßS_i(t)\right)\frac{d}{dt}|S_i(t)|^{\frac{1}{2}}\right\|+n ß\|S_i(t)\|^{\frac{1}{2}}\left\|\dot{S}_i(t)\right\|\right)$$

$$-\lambda_{min}(k_2)\left\|\dot{S}_i(t)\right\|$$

$$\frac{d}{dx}\|\xi_i(t)\| \le \eta n^{3-2\eta}\|(L+G)\otimes I_n\|\|\mathcal{X}(t)\|^{2\eta-1}$$

$$-\lambda_{min}(k_1)\left(\frac{1}{2}\|S_i(t)\|^{\frac{1}{2}}\left\|\dot{S}_i(t)\right\|\left\|tanh\left(ßS_i(t)\right)\right\|+n ß\|S_i(t)\|^{\frac{1}{2}}\left\|\dot{S}_i(t)\right\|\right)$$

$$-\lambda_{min}(k_2)\left\|\dot{S}_i(t)\right\|$$

$$\frac{d}{dx}\|\xi_i(t)\| \le \eta n^{3-2\eta}\|(L+G)\otimes I_n\|\|\mathcal{X}(t)\|^{2\eta-1}$$

$$-\left(\lambda_{min}(k_1)\|S_i(t)\|^{\frac{1}{2}}\left(\frac{1}{2}\left\|tanh\left(ßS_i(t)\right)\right\|+n ß\right)+\lambda_{min}(k_2)\right)\left\|\dot{S}_i(t)\right\|$$

By using assumption 2 and putting the value of $\dot{S}_i(t)$ from (*6.31*):

$$\frac{d}{dx}\|\xi_i(t)\| \le \eta n^{3-2\eta}\mathcal{L}_2\|(L+G)\otimes I_n\|\|\xi_i(t)\| \qquad 6.53$$

$$-\left(\lambda_{min}(k_1)\|S_i(t)\|^{\frac{1}{2}}\left(\frac{1}{2}\left\|tanh\left(ßS_i(t)\right)\right\|+n ß\right)\right.$$

$$\left.+\lambda_{min}(k_2)\right)\left\|\xi_i(t)-k_1\|S_i(t)\|^{\frac{1}{2}}sign\left(S_i(t)\right)-k_2S_i(t)+D_i\right\|$$

$$\frac{d}{dx}\|\xi_i(t)\| \le \gamma_5\|\xi_i(t)\| - \gamma_6\left[\|\xi_i(t)\| - \lambda_{min}(k_1)\|S_i(t)\|^{\frac{1}{2}} - \lambda_{min}(k_2)\|S_i(t)\| + \left\|\mathcal{D}_{i_t}\right\|_\infty\right] \quad 6.54$$

Where $\gamma_5 = \eta n^{3-2\eta}\mathcal{L}_2\|(L+G)\otimes I_n\|$

and $\gamma_6 = \left(\lambda_{min}(k_1)\|S_i(t)\|^{\frac{1}{2}}\left(\frac{1}{2}\left\|tanh\left(ßS_i(t)\right)\right\| + nß\right) + \lambda_{min}(k_2)\right)$. By taking assumption 2 in consideration (*6.54*) can be written as:

$$\frac{d}{dx}\|\xi_i(t)\| \le (\gamma_5 - \gamma_6)\|\xi_i(t)\| + \gamma_6\mathcal{L}_1[\lambda_{min}(k_1) + \lambda_{min}(k_2)]\|x(t)\| - \gamma_6\left\|\mathcal{D}_{i_t}\right\|_\infty$$

Or

$$\frac{d}{dx}\|\xi_i(t)\| \le \gamma_7\|\xi_i(t)\| + \gamma_8\|x(t)\| - \gamma_9\left\|\mathcal{D}_{i_t}\right\|_\infty \quad 6.55$$

Where $\gamma_7 = (\gamma_5 - \gamma_6)$, $\gamma_8 = \gamma_6\mathcal{L}_1[\lambda_{min}(k_1) + \lambda_{min}(k_2)]$ and $\gamma_9 = \gamma_6$.

Solving (*6.55*),

$$\|\xi_i(t)\| \le \vartheta_1 \int_{t_k}^{t} e^{\mu_{\gamma_7}(t-s)}\left[\|x(t)\| + \left\|\mathcal{D}_{i_t}\right\|_\infty\right] ds$$

Where $\vartheta_1 = \max\{\gamma_8, \gamma_9\}$, now by considering $f(t-t_k) = \int_{t_k}^{t} e^{\mu_{\gamma_7}(t-s)} ds$ and using the fact $x(t_k) = x(t) + \frac{1}{\mathcal{L}_1}\xi_i(t)$:

$$\|\xi_i(t)\| \le \frac{\vartheta_1}{\mathcal{L}_1} f(t-t_k)\|\xi_i(t)\| + \vartheta_1 f(t-t_k)\left(\|x(t)\| + \left\|\mathcal{D}_{i_t}\right\|_\infty\right) \quad 6.56$$

Here we assume $f(0) = 0$ & $f(t-t_k)$ is strictly increasing with respect to t, Now for real positive Δ and from (*6.33*) it can be written as:

$$\|\xi_i(t)\| \le \frac{\vartheta_1}{\mathcal{L}_1} f(\Delta)(\sigma\mathcal{L}_1\|x(t)\| + \sigma\mathcal{L}_1\|\mathcal{D}_i\|_\infty) + \vartheta_1 f(\Delta)\left(\|x(t)\| + \left\|\mathcal{D}_{i_t}\right\|_\infty\right) \quad 6.57$$

Or

$$\|\xi_i(t)\| \le \vartheta_1 f(\Delta)(1+\sigma)(\|x(t)\| + \|\mathcal{D}_i\|_\infty) \quad 6.58$$

Comparing (*6.58*) with (*6.33*),

$$f(\Delta) \le \frac{1}{\vartheta_1}\frac{\sigma\mathcal{L}_1}{(1+\sigma)} \quad 6.59$$

Therefore from (*6.59*) any microgrid state control update law such that $\Delta_k \le \Delta$ that

satisfies (*6.33*) for $t \in R_{\geq 0}$. Under the attack of DOS, the main idea is to divide time axis in two intervals, in one-time interval the condition (*6.33*) is satisfied and in another time interval, condition (*6.33*) may not hold due to presence of DOS attack. In this scenario the closed loop microgrid dynamics is to be analyse in a way that it changes in between stable & unstable regions.

Lemma 5 [157]: For an interval $\tau, t \in R_{\geq 0}$, having $0 \leq \tau \leq t$, the duration $[\tau, t]$ is the sum of $\bar{\Theta}(\tau, t)$ & $\bar{\Xi}(\tau, t)$. Here $\bar{\Theta}(\tau, t)$ is representing the interval division of $[\tau, t]$ for which (*6.33*) satisfied whereas, $\bar{\Xi}(\tau, t)$ representing the subinterval of $[\tau, t]$ for which (*6.33*) does not hold. Now, the two real positive sequence of numbers $\langle \zeta_m \rangle_{m \in N_0}$, $\langle v_m \rangle_{m \in N_0}$ are exist in such a way that.

$$\bar{\Xi}(\tau, t) = \bigcup_{m \in N_0} X_m \cap [\tau, t] \tag{6.60}$$

$$\bar{\Theta}(\tau, t) = \bigcup_{m \in N_0} Y_{m-1} \cap [\tau, t] \tag{6.61}$$

With

$$X_m = \langle \zeta_m \rangle \cup [\zeta_m, \zeta_m + v_m[\tag{6.62}$$

$$X_m = \langle \zeta_m + v_m \rangle \cup [\zeta_m + v_m, \zeta_{m+1}[\tag{6.63}$$

and where $\zeta_{-1} = v_{-1} = 0$.

It is noted that in $[\tau, t]$ incorporate the sum of interval ranges $\bar{\Xi}(\tau, t)$ and $\bar{\Theta}(\tau, t)$. Also, the intersection set is empty. Therefore, any successful update of control essentially arises at $\zeta_m + v_m$ by the calculation for each $m \in N_0$, also over the range of Y_m no DOS is present.

In the duration of $Y_m, m \in N_0$, for which the condition (*6.33*) satisfies. From (*6.49*) it is obtained as:

$$\mathcal{V}_1\big(x(t)\big) \leq e^{-\omega_1(t-\zeta_m-v_m)} \mathcal{V}_1\big(x(\zeta_m + v_m)\big) + \gamma_4 \left\| \mathcal{D}_{i_t} \right\|_\infty^2 \tag{6.64}$$

for all time interval $t \in Y_m$ and for all values of $m \in N_0$. The intervals $X_m, m \in N_0$, where the inequality (*6.33*) is not essentially hold true. To design a condition on the rate of enhancement of stability in terms of $\mathcal{V}_1\big(x(t)\big)$, some transitional steps are desired. So, it

can be written for every $m \in N_0$

$$\|\xi_i(t)\| = \|x_{t+k} - x_t\| = \|x_{t+k} - x(\zeta_m) + x(\zeta_m) - x_t\|$$

$$\|\xi_i(t)\| \leq \|x_{t+k} - x(\zeta_m)\| + \|x(\zeta_m)\| + \|x_t\|$$

$$\|\xi_i(t)\| \leq \|\xi_i(\zeta_m)\| + \|x(\zeta_m)\| + \|x_t\|$$

From (*6.33*),

$$\|\xi_i(t)\| \leq \sigma\mathcal{L}_1\|x(\zeta_m)\| + \sigma\mathcal{L}_1\|\mathcal{D}_i(\zeta_m)\|_\infty + \|x(\zeta_m)\| + \|x_t\|$$

Or

$$\|\xi_i(t)\| \leq (1 + \sigma\mathcal{L}_1)\|x(\zeta_m)\| + \|x_t\| + \sigma\mathcal{L}_1\|\mathcal{D}_i\|_\infty \quad 6.65$$

for all $t \in X_m$. Recall that

$$\xi_i(t) \leq \mathcal{L}_1\big(x_i(\zeta_m)\big) - \mathcal{L}_1\big(x_i(\mathrm{t})\big)$$

Here for all time interval of $t \in X_m$, $x(\zeta_m)$ denotes process state the value of the microgrid with the latest successful update of control signal till ζ_m. If suppose $\zeta_0 = 0$, then $x\big(\zeta_m(0)\big) = 0$ in a way (*6.65*) is effective. Eqn. (*6.33*) satisfies for all $t \in Y_m$. therefore, for the microgrid state continuity it can be written as:

$$\|\xi_i(\zeta_m)\| \leq \sigma\mathcal{L}_1\|x(\zeta_m)\| + \sigma\mathcal{L}_1\|\mathcal{D}_i(\zeta_m)\|_\infty \quad 6.66$$

And from the Lyapunov candidate analysis it can be written as:

$$\dot{\mathcal{V}}_1 \leq \mathcal{L}_1\|x(t)\|\|\xi_i(t)\| - \lambda_{min}(k_2)\mathcal{L}_1^2\|x(t)\|^2 + \mathcal{D}_i\mathcal{L}_1\|x(t)\| \quad 6.67$$

Placing (*6.65*) into (*6.67*) results

$$\dot{\mathcal{V}}_1 \leq \mathcal{L}_1\|x(t)\|\big((1 + \sigma\mathcal{L}_1)\|x(\zeta_m)\| + \|x_t\| + \sigma\mathcal{L}_1\|\mathcal{D}_i\|_\infty\big) - \lambda_{min}(k_2)\mathcal{L}_1^2\|x(t)\|^2 + \mathcal{D}_i\mathcal{L}_1\|x(t)\|$$

$$\dot{\mathcal{V}}_1 \leq (1 + \sigma\mathcal{L}_1)\mathcal{L}_1\|x(\zeta_m)\|\|x(t)\| + (\mathcal{L}_1 - \lambda_{min}(k_2)\mathcal{L}_1^2)\|x(t)\|^2 + (\sigma\mathcal{L}_1^2 + \mathcal{L}_1)\|x(t)\|a(t)$$

$$\dot{\mathcal{V}}_1 \leq (1 + \sigma\mathcal{L}_1)\mathcal{L}_1\|x(\zeta_m)\|\|x(t)\| + \gamma_{10}\|x(t)\|^2 + \gamma_{11}\|x(t)\|a(t) \quad 6.68$$

Where, $a(t) := \sup\{\mathcal{D}_i, \|\mathcal{D}_i\|_\infty\}$, $\gamma_{10} = (\mathcal{L}_1 - \lambda_{min}(k_2)\mathcal{L}_1^2)$ and $\gamma_{11} = (\sigma\mathcal{L}_1^2 + \mathcal{L}_1)$.

Now further applying the young's inequality with δ_1 as positive real quantity.

$$2\|x(t)\|a(t) = \frac{1}{\delta_1}\|x(t)\|^2 + \delta_1 a^2(t) \quad 6.69$$

By putting $\delta_1 = \frac{(\sigma\mathcal{L}_1^2 + \mathcal{L}_1)}{(\mathcal{L}_1 - \lambda_{min}(k_2)\mathcal{L}_1^2)}$ *or* $\frac{\gamma_{11}}{\gamma_{10}}$ in (*6.68*), it can be calculated as:

$$\dot{\mathcal{V}}_1 \leq (1+\sigma\mathcal{L}_1)\mathcal{L}_1\|x(\zeta_m)\|\|x(t)\| + \frac{3\gamma_{10}}{2}\|x(t)\|^2 + \frac{{\gamma_{11}}^2}{2\gamma_{10}}a^2(t) \quad 6.70$$

Or

$$\dot{\mathcal{V}}_1 \leq \gamma_{12}\|x(\zeta_m)\|\|x(t)\| + \frac{3\gamma_{10}}{2}\|x(t)\|^2 + \frac{{\gamma_{11}}^2}{2\gamma_{10}}a^2(t) \quad 6.71$$

Where $\gamma_{12} = (1+\sigma\mathcal{L}_1)\mathcal{L}_1$.

Now again repeating the sequence of applying young's inequality with δ_2 as positive real quantity.

$$2\|x(\zeta_m)\|\|x(t)\| = \frac{1}{\delta_2}\|x(t)\|^2 + \delta_2\|x(\zeta_m)\|^2 \quad 6.72$$

By putting $\delta_2 = \frac{(1+\sigma\mathcal{L}_1)\mathcal{L}_1}{(\mathcal{L}_1 - \bar{\lambda}_{min}(k_2)\mathcal{L}_1^2)}$ *or* $\frac{\gamma_{12}}{\gamma_{10}}$ in (*6.68*), it can be calculated as:

$$\dot{\mathcal{V}}_1 \leq 2\gamma_{10}\|x(t)\|^2 + \frac{{\gamma_{12}}^2}{2\gamma_{10}}\|x(\zeta_m)\|^2 + \frac{{\gamma_{11}}^2}{2\gamma_{10}}a^2(t) \quad 6.73$$

as $\|a_t\|_\infty = \left\|\mathcal{D}_{i_t}\right\|_\infty$ for $t \in R_{\geq 0}$, and $\gamma_{13} = \frac{{\gamma_{11}}^2}{2\gamma_{10}}$ then it can be written as:

$$\dot{\mathcal{V}}_1 \leq 2\gamma_{10}\|x(t)\|^2 + \frac{{\gamma_{12}}^2}{2\gamma_{10}}\|x(\zeta_m)\|^2 + \gamma_{13}\left\|\mathcal{D}_{i_t}\right\|_\infty^2 \quad 6.74$$

Now from (*6.46*) and (*6.74*) it can be written as:

$$\dot{\mathcal{V}}_1 \leq \omega_2\, max\{\mathcal{V}_1(x(t)), \mathcal{V}_1(x(\zeta_m))\} + \gamma_{13}\left\|\mathcal{D}_{i_t}\right\|_\infty^2 \quad 6.75$$

Where, the value of parameter related to divergence rate of system stability in presence of DOS ω_2 is obtained as:

$$\omega_2 = \frac{2\gamma_{10}}{\alpha_1\mathcal{L}_1} \quad 6.76$$

And

$$\dot{\mathcal{V}}_1 \leq e^{\omega_2(t-\zeta_m)}\mathcal{V}_1(x(\zeta_m)) + \gamma_{14}e^{\omega_2(t-\zeta_m)}\left\|\mathcal{D}_{i_t}\right\|_\infty^2 \quad 6.77$$

for $t \in X_m$, with $\gamma_{14} = \frac{\gamma_{13}}{\omega_2}$.

6.6 Verification and result analysis of the proposed scheme

The resilient control design for the multi-DG based microgrid network under DOS attack in section 6.3 is validated in the MATLAB/Simulink platform. For the validation of the control strategy, four DG based microgrid structure shown in Figure *6.1* is considered for the simulation purpose. The respective parameters describing the microgrid specification are presented in the Table 6.1. This control scheme concerns the cooperative secondary voltage frequency control in islanded mode of operation of the microgrid under the threat of cyber-attack. DOS attack sequence is scheduled from the source block set taken as random interrupt signal that is incorporated through the programming under the communication graph theory.

SYSTEM PROPERTIES AND SPECIFICATIONS

	SYMBOLS	DG1	DG2	DG3	DG4
DGs	m_P	0.0000 78	0.0000 67	0.0000 67	0.000 054
	n_Q	0.0015	0.0013	0.0013	0.001 1
Lines	Z_1, Z_3		$0.15 + j0.1$		
	Z_2		$0.70 + j0.84$		
	Z_4, Z_5		$0.35 + j0.42$		
RL-Load	Load-bus1,2		$320 + j0.48$		
	Load-bus3,4		$250 + j0.95$		
Gains	k_1, k_2	1.43, 2.21	1.18, 3.10	1.22, 2.09	1.8, 3.31
	λ		1.2		

Table 6.1. System Properties and Specifications

6.6.1. Simulation results obtained from the proposed scheme and discussion.

Four DG based microgrid structure shown in Figure *6.1* is simulated in MATLAB/Simulink with the specification given in the Table 6.1 under the DOS attack. The DOS sequences as generated randomly through the communication graph theory on the secondary control channel connected with all DGs of the network microgrid. The DOS attack duration is represented by the gray color bars plots in Figure *6.4* and Figure *6.5*. Under the impact of DOS different results with respect to microgrid parameter state variations are obtained that are shown from Figure *6.4* to Figure *6.10*. The variation in the frequency

(ω) of each DG connected to the microgrid is depicted in Figure *6.4*. The variation in the direct bus voltage of each DG is shown in the Figure *6.5*.

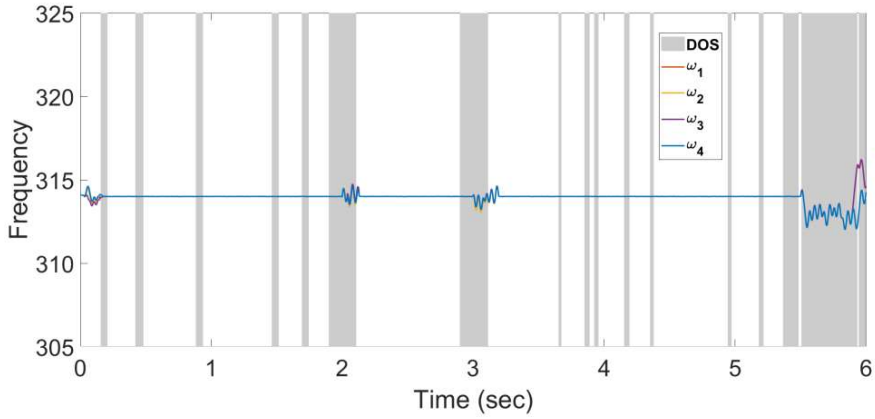

Figure 6.4. Impact on the Bus frequencies of the microgrid Under DOS attack.

Both the Figure *6.4* and Figure *6.5* incorporates the sequence of DOS. After the initial transient these secondary microgrid states are stabilized under the sliding mode-based consensus control, but due to the occurrence of DOS these states are perturbed from their stabilized equilibrium at the duration of DOS beyond the stability bound. At the time of high DOS duration at 2 and 3 sec the states are deviated but the impact of DOS is in the tolerable limit. These states at 2 and 3 sec are stabilized after the DOS active duration. Small duration of the DOS is tolerable to an extent. As it can be seen from the results when the duration of DOS is highly increased all microgrid states under secondary operation gets deviated from the stable trajectory as seen after 5.5 sec in the Figure *6.4* and Figure *6.5*.

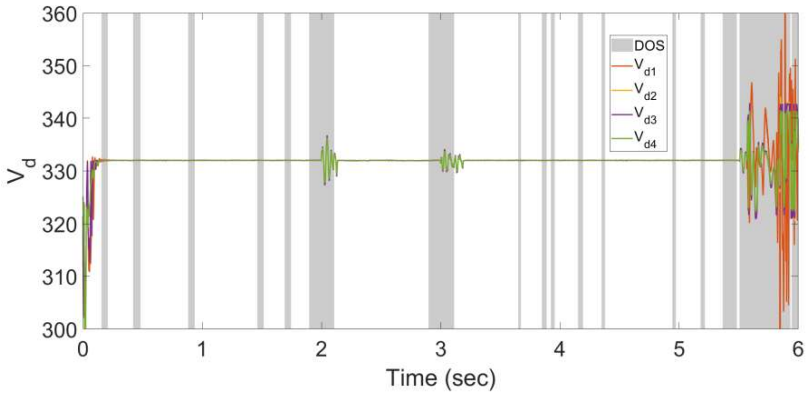

Figure 6.5. Impact on the direct voltages at each bus of the microgrid Under DOS attack.

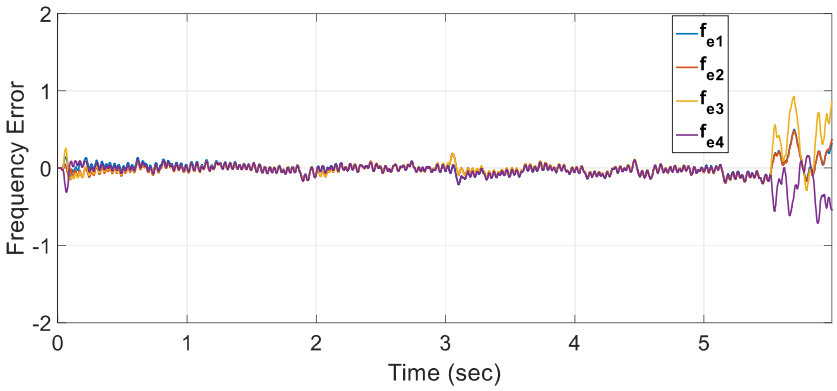

Figure 6.6. Impact on the consensus-based frequency error of the microgrid Under DOS attack.

Figure 6.6 shows the consensus error plot of the frequency corresponding to all DGs connected to the microgrid. At each DOS event the deviation in the respective error between DG configuration is observed under violation of stability bounds at 2 and 3 sec. After the active duration of DOS, error states are stabilized at 2 and 3 sec. In the case of large DOS duration, the deviation of error is abruptly deteriorated. The similar results are obtained for the consensus-based direct voltage error of the network microgrid as illustrated in *Figure 6.7*.

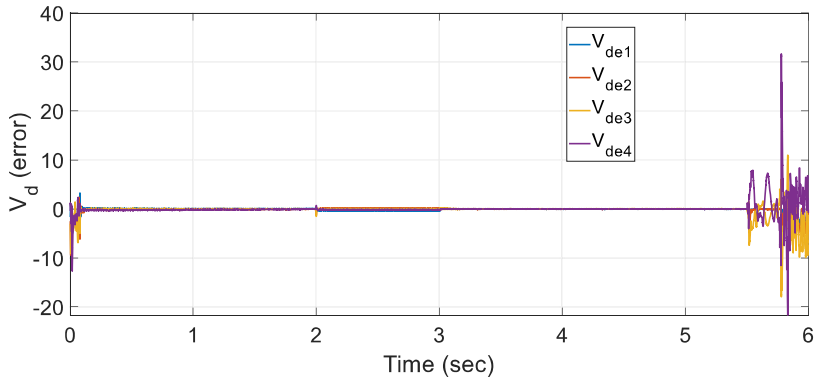

Figure 6.7. Impact on the consensus-based voltage error of the microgrid Under DOS attack.

The impact of DOS sequence can be analyzed on the quadrature component of the bus voltages from the Figure *6.8*. All DGs quadrature components are shown in the Figure *6.8*. The corresponding deviation due to DOS is reflected in the quadratic components of the bus voltages at 2 and 3 sec. Also, after 5.5 sec the quadratic voltage components deteriorate. DOS impact on the corresponding rated DG powers in the droop ratio with the frequency is shown in the Figure *6.9*. Deviations at 2 and 3 sec are observed that are

further stabilized as per the deactivated DOS duration. Unstable power states region is seen after 5.5 sec due to high impact of DOS.

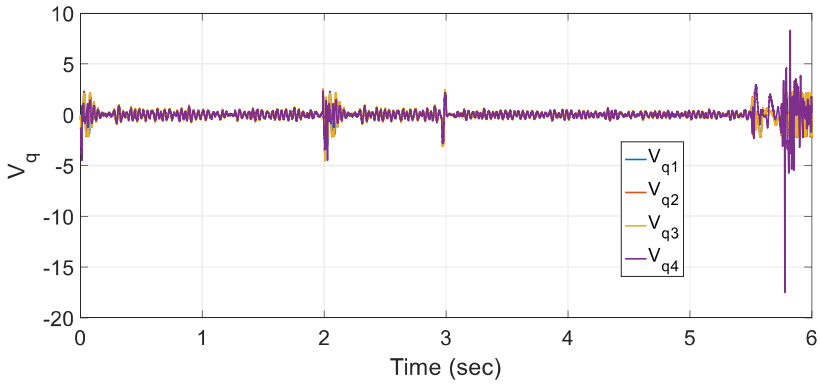

Figure 6.8. Impact on the quadrature component of the bus voltages of the microgrid Under DOS attack.

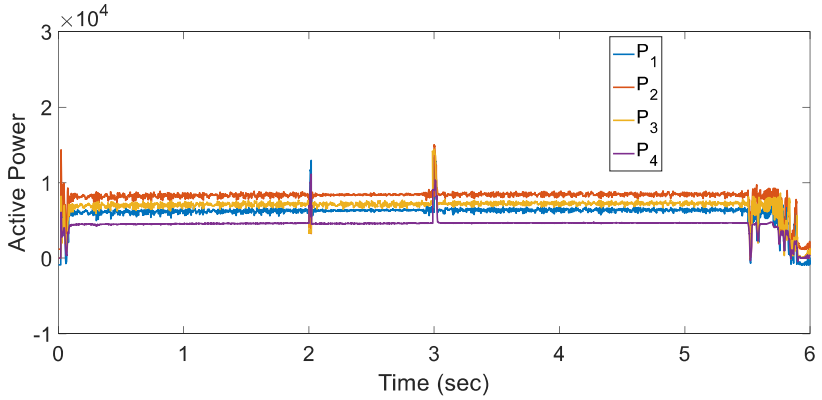

Figure 6.9. Impact on the bus active powers of each DG in the microgrid Under DOS attack.

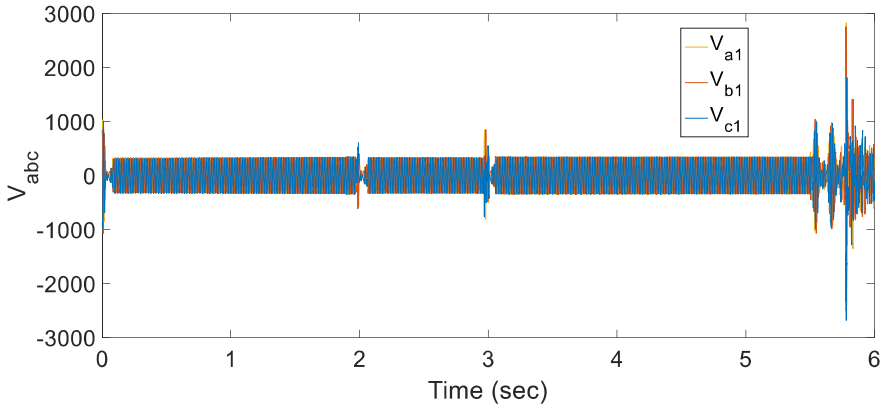

Figure 6.10. Impact on the $3-\emptyset$ bus voltage of DG2 Under DOS attack.

The three-phase voltage at bus 2 under DOS attack is shown in the Figure *6.10*. Here, the similarity with the other microgrid states is observed as per the sequence of DOS attack. Stability region, deviation of three phase voltage at 2 & 3 sec and deterioration of the

voltage after 5.5 sec can be seen from the result shown in Figure *6.10*.

6.7 Summary

The proposed control scheme shows robust performance with minimal control effort in the microgrid structure under DOS attack. The stability in terms of Lyapunov candidature is proved with the analysis of DOS frequency and duration for which closed loop microgrid stability remains preserved. Under DOS attack stability in terms of converging and diverging parameters is discussed by division of sub intervals of the DOS attack sequence with the on-off jamming ratio. The multi-DG based microgrid control strategy is governed by sliding mode control design that provides the sampling rule for which ISS of the microgrid system is achieved and its robustness against system disturbance is ensured. Further the DOS attack resilient control algorithm is applied on the secondary voltage/frequency control of the microgrid. From the obtained results it is observed that all microgrid states under attack are stabilized to an extent of stability bounds over which the deterioration of the microgrid states is started. DOS tolerance limit is determined by the relevant triggering-based control design using sliding mode. Pertaining to this control design for microgrid effect of delay in information exchange can be the future scope of the work. As a matter of fact, results verify the objective of proposed technique for autonomous ac microgrid operating in islanded mode of operation.